PROCEEDINGS A

Research

CrossMark
click for updates

Whitham modulation theory for the Ostrovsky equation

A. J. Whitfield[1] and E. R. Johnson[2]

[1,2]Department of Mathematics, University College London, London, WC1E 6BT, United Kingdom

This paper derives the Whitham modulation equations for the Ostrovsky equation. The equations are then used to analyse localised cnoidal wavepacket solutions of the Ostrovsky equation in the weak rotation limit. The analysis is split into two main parameter regimes: the Ostrovsky equation with normal dispersion relevant to typical oceanic parameters and the Ostrovsky equation with anomalous dispersion relevant to strongly sheared oceanic flows and other physical systems. For anomalous dispersion a new steady, symmetric cnoidal wavepacket solution is presented. The new wavepacket can be represented as a solution of the modulation equations and an analytical solution for the outer solution of the wavepacket is given. For normal dispersion the modulation equations are used to describe the unsteady finite-amplitude wavepacket solutions produced from the rotation-induced decay of a Korteweg-de Vries solitary wave. Again, an analytical solution for the outer solution can be given. The centre of the wavepacket closely approximates a train of solitary waves with the results suggesting that the unsteady wavepacket is a localised, modulated cnoidal wavetrain. The formation of wavepackets from solitary wave initial conditions is considered, contrasting the rapid formation of the packets in anomalous dispersion with the slower formation of unsteady packets under normal dispersion.

THE ROYAL SOCIETY
PUBLISHING

1. Introduction

Oceanic internal waves are often assumed to have amplitudes small compared with the depth (weak nonlinearity) and wavelengths long compared with the depth (weak dispersion). Under these assumptions the Korteweg-de Vries (KdV) equation

$$u_t + uu_x + u_{xxx} = 0, \tag{1.1}$$

gives an accurate description for the interfacial displacement of the waves [1, 2, 3, 4]. In KdV-type theories the effects of background rotation are often considered negligible although observed waves can persist for several days allowing rotational effects to become important. The simplest extension of the KdV equation that takes the effects of rotation into account is the Ostrovsky (rotation-modified KdV) equation [5]

$$u_t + uu_x + u_{xxx} = \gamma \int_{-\infty}^{x} u \, dx', \tag{1.2}$$

where γ represents the relative strength of background rotation. An interesting feature of the Ostrovsky equation is the zero-mass constraint for localised solutions,

$$\int_{-\infty}^{\infty} u \, dx = 0. \tag{1.3}$$

The Ostrovsky equation is only applicable in the finite range of wavenumbers that excludes the zero wavenumber [6]. The constraint (1.3) is equivalent to the requirement that the solution has no energy at the zero wavenumber, which is consistent with the derivation of the Ostrovsky equation.

The effect of adding the nonlocal integral term to the right hand side of the KdV equation is to introduce "large-scale" dispersion into the system. For oceanic waves, the coefficient representing the strength of rotation is usually positive, $\gamma > 0$, and this parameter regime has been described as the Ostrovsky equation with normal dispersion [7]. The opposite case, when $\gamma < 0$, arises in strongly-sheared ocean flows and acoustic problems [7] and is described as anomalous dispersion.

In the strong-rotation limit ($\gamma \gg 1$) it has been shown that the Ostrovsky equation supports localised wavepacket solutions for both cases of dispersion and several recent articles [7, 8, 9, 10] have examined the dynamics of these wavepackets. In the weak-rotation limit ($\gamma \ll 1$), wavepackets have been observed for normal dispersion only. Helfrich [11], who was the first to discover these rotation induced wavepackets, originally stated the solutions resemble modulated cnoidal wave train solutions of the KdV equation, however these observations remain currently unexplained.

For the unperturbed KdV equation (1.1), it is possible to derive a set of equations that describe the evolution of a modulated cnoidal wave train in the limit of no dispersion. In the literature these equations are often referred to as the Whitham modulation equations [12]. The derivation is a direct consequence of the property that the KdV equation is completely integrable. The Ostrovsky equation is not integrable and hence it is not possible to derive a similar set of equations.

Myint and Grimshaw [13] formulated a way of deriving the modulation equations for a KdV equation with a perturbation term,

$$u_t + uu_x + u_{xxx} = \epsilon \, V(u), \tag{1.4}$$

where $V(u)$ is an arbitrary functional of u and $\epsilon \ll 1$. Kamchatnov [14] has generalised their results but applying this work to the Ostrovsky equation is not direct because of the atypical nature of the non-local perturbation term.

This paper makes some minor changes to the method of Myint and Grimshaw [13] to derive a set of modulation equations for the Ostrovsky equation. Section 2 sketches briefly the derivation of the perturbed modulation equations which are verified against numerical integrations of the Ostrovsky equation. The derived equations are then used in §3 to describe wavepacket solutions

of the Ostrovsky equation with §3(a) considering steady wavepacket solutions with anomalous dispersion and §3(b) unsteady wavepacket solutions with normal dispersion. Section 4 addresses the emergence of these wavepackets and in particular the rapid formation of packets under anomalous dispersion in contrast to their slower formation under normal dispersion.

2. Derivation of the modulation equations

Let the perturbative rotational term in the Ostrovsky equation be of order ϵ^2 and take the derivative of equation (1.2) so that it is in the form

$$(u_t + uu_x + u_{xxx})_x = \pm\epsilon^2 u, \tag{2.1}$$

where $\epsilon > 0$ and the positive and negative signs refer to normal and anomalous dispersion respectively. If a solution of (2.1) has period $2L$, is of compact support lying in $|x| < L$, or decays sufficiently rapidly as $x \to \pm\infty$ then it satisfies the zero mass condition

$$\int_{-L}^{L} u \, \mathrm{d}x = 0, \tag{2.2}$$

where L is infinite in the last case.

Following Myint and Grimshaw [13] the equations governing modulated nonlinear wavetrain solutions of (2.1) can be derived straightforwardly by and seeking a solution of the form

$$u(x, t) = u_0(\theta, X, T) + \epsilon u_1(\theta, X, T) + \epsilon^2 u_2(\theta, X, T) + \cdots, \tag{2.3}$$

where the fast variable θ and the slow space and time variables X and T are defined as

$$\theta = \epsilon^{-1}\Theta(X, T), \qquad X = \epsilon x, \qquad T = \epsilon t. \tag{2.4}$$

The local frequency $\omega(X, T)$, local wavenumber $k(X, T)$ and local phase velocity $c(X, T)$ are defined by

$$\omega = -\Theta_T, \qquad k = \Theta_X, \qquad \omega = kc, \tag{2.5}$$

and are related by the consistency condition,

$$k_T + (kc)_X = 0, \tag{2.6}$$

describing the conservation of waves.

Let the modulations be periodic with period $2L$, or of compact support lying in $|X| < L$, or decay sufficiently rapidly as $X \to \infty$, then an anti-differentiation operator ∂_X^{-1} can be defined such that for any function $v(X)$,

$$\partial_X^{-1} v = -\int_X^L v(X') \mathrm{d}X', \tag{2.7}$$

with L infinite in the last case. If, further, v satisfies (2.2) then

$$\partial_X^{-1} v = 0 \text{ at } X = \pm L. \tag{2.8}$$

It is convenient to divide both sides of (1.2) by ϵ to give

$$(u_t + uu_x + u_{xxx})_X = \pm\epsilon u, \tag{2.9}$$

and so

$$u_t + uu_x + u_{xxx} = \pm\epsilon\partial_X^{-1} u, \tag{2.10}$$

for solutions vanishing as $x \to \infty$. Then substituting (2.3) into (2.9) gives at leading order

$$(-kcu_{0\theta} + ku_0 u_{0\theta} + k^3 u_{0\theta\theta\theta})_X = 0. \tag{2.11}$$

Equation (2.11) can be integrated once to give

$$(-kcu_0 + \frac{1}{2}ku_0^2 + k^3 u_{0\theta\theta})_\theta = C(T), \tag{2.12}$$

for some function $C(T)$. Let the period in θ of the carrier waves making up the wavetrain be $2P$. Then integrating (2.12) over a period $2P$ in θ and using the periodicity of u_0 shows that $C(T)$ is identically zero. Hence (2.11) can be written,

$$-cu_{0\theta} + u_0 u_{0\theta} + k^2 u_{0\theta\theta\theta} = 0. \tag{2.13}$$

Using (2.10) allows the next term in the expansion to be written as

$$-kcu_{1\theta} + k(u_0 u_1)_\theta + k^3 u_{1\theta\theta\theta} + f_1 = 0, \tag{2.14}$$

where

$$f_1 = u_{0T} + u_0 u_{0X} + 3k^2 u_{0\theta\theta X} + 3kk_X u_{0\theta\theta} \mp \partial_X^{-1} u_0. \tag{2.15}$$

Integrating (2.14) with respect to θ over a period $2P$, and using the periodicity of u_1, gives

$$\langle f_1 \rangle = 0, \tag{2.16}$$

where the mean of any $2P$-periodic function $v(\theta)$ is defined as

$$\langle v \rangle = \frac{1}{2P} \int_{-P}^{P} v(\theta) \mathrm{d}\theta. \tag{2.17}$$

Multiplying (2.14) by u_0, integrating with respect to θ over a period $2P$, and using periodicity and the fact that u_0 satisfies (2.13), gives

$$\langle u_0 f_1 \rangle = 0. \tag{2.18}$$

This averaging operator also gives a simpler form for the anti-differentiation operator. For any function $v(\theta, X)$ of the slowly-varying X and rapidly varying θ, of period $2P$ in θ,

$$\int_{X_1}^{X_2} v \mathrm{d}X = \int_{X_1}^{X_2} [\langle v \rangle + (v - \langle v \rangle)] \mathrm{d}X = \int_{X_1}^{X_2} \langle v \rangle \mathrm{d}X, \tag{2.19}$$

since the second term in the second integral vanishes in every consecutive sub-interval of length $2P$ in θ from the construction of $\langle v \rangle$. Thus

$$\partial_X^{-1} v = \partial_X^{-1} \langle v \rangle, \tag{2.20}$$

which is a slowly-varying function, unaffected by further averaging.

Combined with the consistency relation (2.6), equations (2.16) and (2.18) give the modulation equations for the leading order solution u_0. The remainder of the analysis is confined to this leading order solution and since the modulation equations form a closed system the subscript zero can be dropped without ambiguity. Substituting for f_1 in (2.16) and (2.18) then using (2.20) gives

$$\langle u \rangle_T + \frac{1}{2} \langle u^2 \rangle_X = \pm \partial_X^{-1} \langle u \rangle, \tag{2.21a}$$

$$\frac{1}{2} \langle u^2 \rangle_T + \frac{1}{3} \langle u^3 \rangle_X - \frac{3}{2} (k^2 \langle u_\theta^2 \rangle)_X = \pm \langle u \partial_X^{-1} \langle u \rangle \rangle. \tag{2.21b}$$

These equations are precisely those of Myint and Grimshaw [13] with the operator $V(u)$ replaced by integration with respect to X, the slow-x variable.

Equation (2.13) has the exact periodic cnoidal solution,

$$u = a\{b + \mathrm{cn}^2[\beta(\theta - \theta_0)]\} + d, \tag{2.22}$$

where cn is the Jacobi elliptic function with parameter m (described in [13] as the modulus, usually used for $m^{1/2}$). Choose b so that d is the mean value of u, i.e. $d = \langle u \rangle$, then

$$a = 12mk^2\beta^2, \tag{2.23a}$$

$$b = (1 - m)/m - E(m)/mK(m), \tag{2.23b}$$

$$c = d + (a/3m)[2 - m - 3E(m)/K(m)], \tag{2.23c}$$

$$P = K(m)/\beta. \tag{2.23d}$$

and all parameters are slowly varying functions such that $a(X, T)$, $b(X, T)$, $c(X, T)$, $d(X, T)$, $k(X, T)$, $m(X, T)$ and $\beta(X, T)$. The phase shift $\theta_0(X, T)$ cannot be determined without considering the second-order terms in the expansion (2.3), but as its value does not affect the other parameters it is ignored in the subsequent analysis.

Integrating (2.13) twice with respect to θ gives

$$k^2 u_\theta^2 = 2A + 2Bu + cu^2 - u^3/3, \tag{2.24}$$

where

$$A = -(ab + d)^3/3 + c(ab + d)^2/2 - a^2(1 - m)(ab + d)/6m, \tag{2.25a}$$

$$B = (ab + d)^2/2 - c(ab + d) + a^2(1 - m)/6m. \tag{2.25b}$$

Differentiating (2.24) with respect to θ and dividing by $2u_\theta$ gives

$$k^2 u_{\theta\theta} = B + cu - u^2/2, \tag{2.26}$$

and averaging (2.26) gives, for the cnoidal solution,

$$\langle u^2 \rangle = 2(B + c\langle u \rangle) = 2(B + cd). \tag{2.27}$$

Multiplying (2.26) by u and averaging gives,

$$-k^2 \langle u_\theta^2 \rangle = Bd + c\langle u^2 \rangle - \langle u^3 \rangle/2, \tag{2.28}$$

whereas averaging (2.24) directly gives

$$k^2 \langle u_\theta^2 \rangle = 2A + 2Bd + c\langle u^2 \rangle - \langle u^3 \rangle/3. \tag{2.29}$$

Then adding (2.28) and (2.29) gives

$$(5/6)\langle u^3 \rangle = 2A + 3Bd + 2c\langle u^2 \rangle, \tag{2.30}$$

and taking $3 \times$ (2.29) – 2 (2.28) gives

$$5k^2 \langle u_\theta^2 \rangle = 6A + 4Bd + c\langle u^2 \rangle. \tag{2.31}$$

Substituting (2.22) in system (2.21) and including the consistency relation (2.6) gives the required modulation equation system

$$k_T + (ck)_X = 0, \tag{2.32a}$$

$$d_T + (cd + B)_X = \pm\partial_X^{-1}d, \tag{2.32b}$$

$$(cd + B)_T + [c(cd + B) - A]_X = \pm(1/2)[(\partial_X^{-1}d)^2]_X. \tag{2.32c}$$

using $d(\partial_X^{-1}d) = (1/2)[(\partial_X^{-1}d)^2]_X$. Since there are four equations (2.23a-d) between the seven parameters a, b, c, d, k, m, β only three are independent and hence equations (2.32a-c) are sufficient to determine the solution.

Following Whitham [12], the equations (2.32a-c) can be greatly simplified introducing the variables,

$$r_1 = q + r, \quad r_2 = r + p, \quad r_3 = p + q, \tag{2.33}$$

where p, q, r, $(r \leq q \leq p)$ given by,

$$p = d + (a/m)[1 - E(m)/K(m)], \tag{2.34a}$$

$$q = d + (a/m)[1 - m - E(m)/K(m)], \tag{2.34b}$$

$$r = d - (a/m)[E(m)/K(m)], \tag{2.34c}$$

are the three roots of the polynomial on the right hand side of (2.24). The modulation equations (2.32) can be written,

$$r_{iT} + Q_i(r_1, r_2, r_3)r_{iX} = \pm 2(\partial_X^{-1} d), \quad \text{for} \quad i = 1, 2, 3, \tag{2.35}$$

where each r_i is a Riemann invariant that propagates with characteristic velocity Q_i, given by

$$Q_1 = c - (a/3)[K(m)/(K(m) - E(m))] \tag{2.36a}$$

$$Q_2 = c - (a/3)(1 - m)K(m)/[E(m) - (1 - m)K(m)] \tag{2.36b}$$

$$Q_3 = c + (a/3)(1 - m)K(m)/[mE(m)]. \tag{2.36c}$$

The change of variables required to derive equations (2.35) from equations (2.32) is laborious (details can be found in [12, 13]).

As a function of the Riemann invariants, the solution (2.22) takes the form,

$$u = (r_1 + r_2 - r_3)/2 + (r_2 - r_1)\operatorname{cn}^2[\sqrt{(r_3 - r_1)/12}(\xi - \xi_0)], \tag{2.37}$$

where,

$$\xi = x - ct, \quad c = (r_1 + r_2 + r_3)/6, \quad m = (r_2 - r_1)/(r_3 - r_1), \tag{2.38}$$

and ξ_0 is a phase shift. The wavelength $\lambda = 2P/k$ is given by

$$\lambda = 2K(m)/\sqrt{(r_3 - r_1)/12}, \tag{2.39}$$

and the maximum and minimum values of u are

$$u_{max} = (r_2 + r_3 - r_1)/2 \quad \text{and} \quad u_{min} = (r_1 + r_3 - r_2)/2. \tag{2.40}$$

The wave amplitude and mean of u are given by

$$a = r_2 - r_1 \quad \text{and} \quad d = (r_1 + r_2 - r_3)/2 + (r_3 - r_1)E(m)/K(m). \tag{2.41}$$

To test the results derived above, both the Ostrovsky equation (2.1) and equations (2.35) were integrated numerically with equivalent initial conditions. To integrate both the modulation equations (2.35) and the Ostrovsky equation (2.1) a pseudo-spectral Fourier discretization on a periodic domain in x and an adaptive 4th-order Runge-Kutta time-stepping in t was used. The initial condition was chosen as a cnoidal wavetrain (2.22) with $a = 1 + 0.5\exp[-x^2/150]$, $d = 0$ and $m = 0.97$. Figure 1 shows the results of the integration. The solutions obtained from integrating the Ostrovsky equation are shown by the solid lines and the envelope solutions obtained from integrating the modulation equations are shown by the dashed lines. Figure 1(a) shows the solution used for both integrations at $t = 0$. Figure 1(b) shows a comparison of the integrations at $t = 325$ when no large-scale dispersion is present. This case corresponds to the KdV equation and unperturbed Whitham modulation equations. Figure 1(c) shows a comparison of the integrations at $t = 325$ for normal dispersion of magnitude $\epsilon = 0.1$ and figure 1(d) shows a comparison of the integrations at $t = 300$ for anomalous dispersion of magnitude $\epsilon = 0.224$.

The solutions of the perturbed modulation equations agree qualitatively with the corresponding integrations of the Ostrovsky equation. The modulation equations, however, are only valid for sufficiently small ϵ (≈ 0.1). It should be noted that for larger ϵ, the KdV equation cnoidal wave (2.22) is no longer an approximate solution of the Ostrovsky equation and the theory

becomes invalid. This is demonstrated in figure 1(d) where $\epsilon = 0.224$. The wavetrain to the left of the disturbance no longer appears cnoidal.

A striking feature of the integrations shown in figure 1 is that the modulation equations appear to correctly capture the nonlinear steeping behaviour exhibited when either normal or anomalous dispersion are present (figures 1(c-d)). Furthermore for the normal dispersion case in figure 1(c) the three peaked structure located between $x = -200$ and -300 loosely resembles that of the rotation-induced wavepackets seen in [8, 9, 11].

3. Application to wavepackets

(a) Anomalous dispersion

For anomalous dispersion, it is known steady localised solutions exist. In the strong-rotation limit ($\epsilon \gg 1$) these solutions originate from the point in wavenumber space where the linear phase and group velocities are equal [7], but as the strength of rotation is decreased the wavepacket structure of this family of solutions is eventually replaced by a soliton solution (figure 2(a)) that is described asymptotically by a KdV soliton with pedestal of order $\epsilon \ll 1$ [15].

Section 4 describes how these single-peak solitary wave solutions arise naturally from the evolution of an initial KdV soliton in the presence of weak rotation. These are not however the only steadily-propagating solutions of compact support. Figures 2(b), (c) show new steady wavepacket solutions found by a spectral Newton-Kantorovich iteration on a periodic grid.

The packet in figure 2(b) has the form of three adjacent KdV solitons. The packet in figure 2(c) resembles neither figure 2(a) nor (b). It was found that as more peaks were added to the solution the leading and trailing edges retained the form of solitary waves but the centre of the packet became more sinusoidal. It was also found that solutions with more peaks could only be obtained by decreasing the strength of rotation. Additionally the velocity and rotation strength of the solutions in figure 2 are related such that $c = 20\epsilon/3$ by construction. An approximation for the envelopes of the multi-peak solutions were found using numerical interpolation of the peaks and troughs. It was observed that the maximum of the lower envelope occurred at the centre of the packet and approached zero as the number of peaks increased, a result that is derived later on in this section. Note that the small peak number (stronger rotation) limit of the solution family shown here coincides with the first member of the solution family shown in figure 4 of Obregon and Stepanyants [16], found by placing two individual solitons (similar to figure 2(a)) at the local maxima of each other, but at stronger rotation strengths than are considered here.

For an anomalous wavepacket moving at constant velocity c_0, the time dependence of the modulation equations (2.35) can be removed by introducing the variables $r_i = r_i'(X')$, $Q_i = Q_i'(X')$, $d = d'(X')$ where $X' = X - c_0 T$. Substituting the new variables into (2.35) and dropping dashes gives

$$\frac{\mathrm{d}r_i}{\mathrm{d}X} = -\frac{2D}{(Q_i - c_0)}, \quad \text{where} \quad \mathrm{d}D/\mathrm{d}X = d. \tag{3.1}$$

If the wavepacket is steady, i.e. $c = c_0$, one of the Riemann invariants, r_i, can be eliminated using (2.38). Further if the packet is assumed to be symmetric, forcing $D(0) = 0$, then integrating equation (2.32c) after transforming into the frame, $X' = X - c_0 T$, shows that

$$D = \mathrm{sgn}(X)\sqrt{2(A - A_0)}, \tag{3.2}$$

where $A_0 = A(0)$ and $\mathrm{sgn}(X)$ is the signum function. The sign of the root in (3.2) has been chosen to agree with packets like that those shown in figure 2 where the "mass" is initially negative when approaching the packet from negative x. Hence for a steady, localised, symmetric wavepacket the modulation equations are reduced to a set of two ordinary differential equations.

To test if the modulation equations have wavepacket solutions, equations (3.1) were integrated numerically using an initial condition corresponding to the wavepacket solution shown in figure 2(c). An approximation for the envelope of the solution in figure 2(c) was found using numerical interpolation of the peaks and troughs. Using the known velocity c_0 and equations (2.40) and
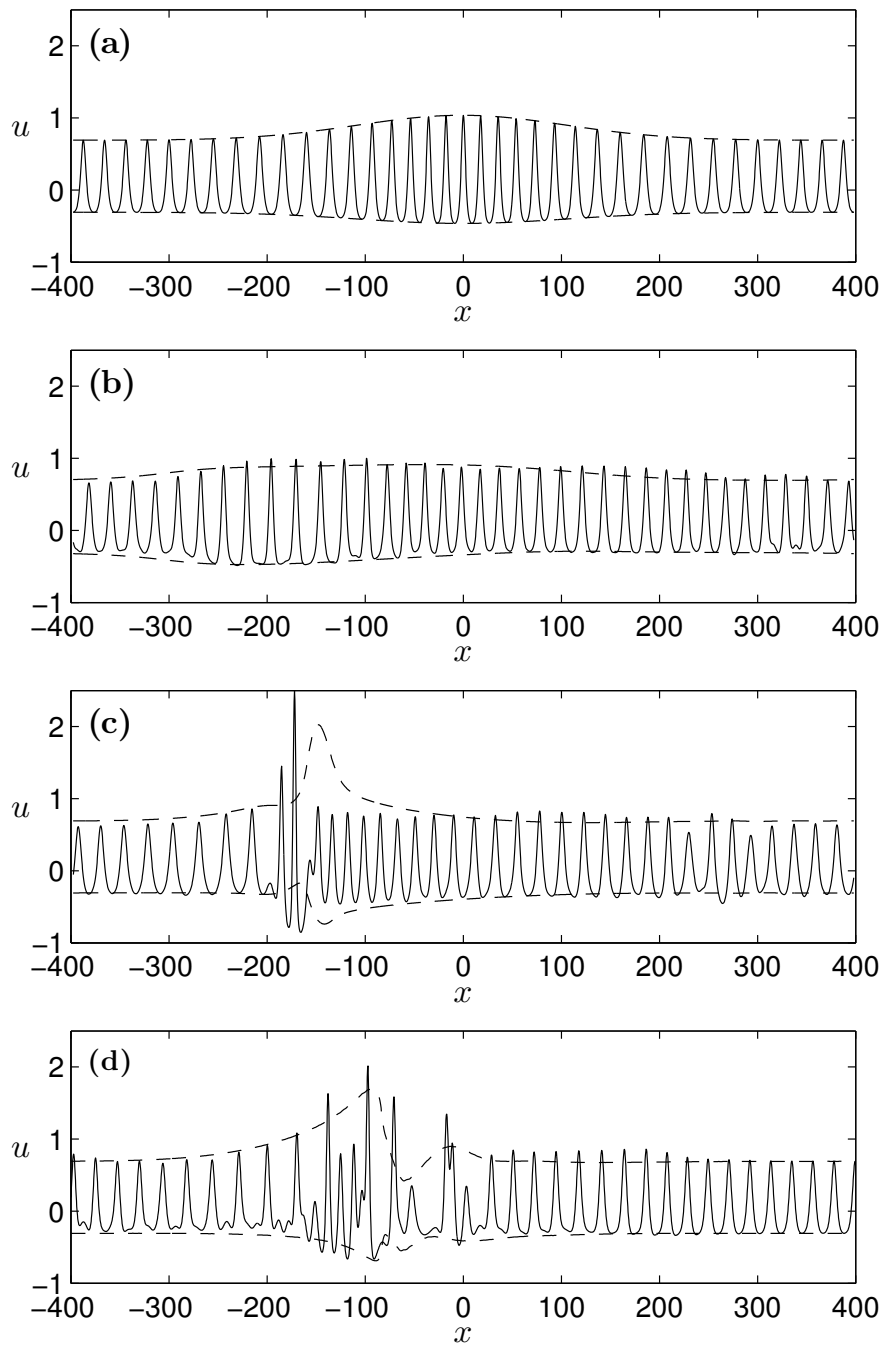
Figure 1. Numerical integrations of the Ostrovsky equation (solid lines) and the time-dependent modulation equations (dashed lines) for both normal and anomalous dispersion. (a) A cnoidal initial condition with parameters $a = 1 + 0.5 \exp[-x^2/150]$, $d = 0$ and $m = 0.97$. (b) Integrations for the unperturbed case $\epsilon = 0$ at $t = 325$. (c) Integrations for normal dispersion $\epsilon = 0.1$ at $t = 325$ (d) Integrations for anomalous dispersion $\epsilon = 0.224$ at $t = 300$.

(2.41), approximations for $r_1(0)$ and $r_2(0)$ were then found. Rather than use the analytical expression for D given in equation (3.2), the equation $\mathrm{d}D/\mathrm{d}X = d$ was used, to avoid the difficulty of integrating from a stationary point.
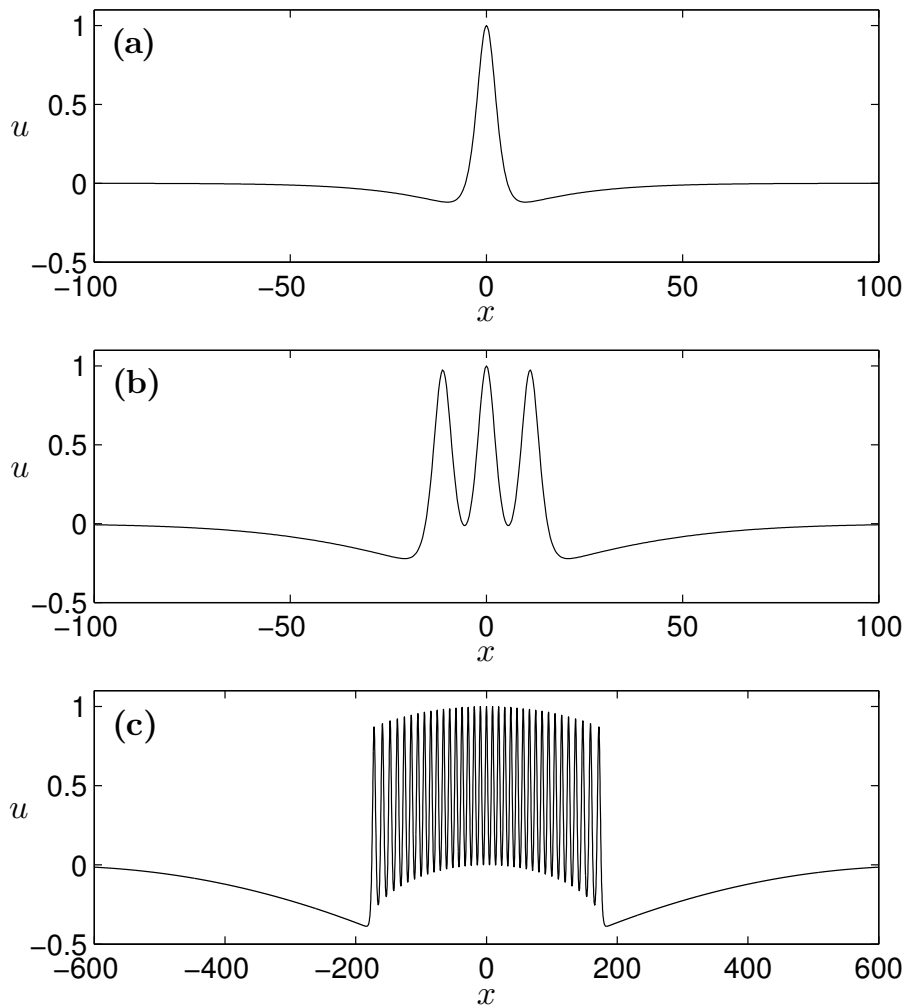
Figure 2. Numerical solutions of the Ostrovsky equation with anomalous dispersion moving at constant velocity $c = c_0$. (a) A soliton solution with $\epsilon = 0.0324$ and $c_0 = 0.213$. (b) A 3-peak packet solution with $\epsilon = 0.0207$ and $c_0 = 0.138$. (c) A 35-peak packet solution with $\epsilon = 0.00320$ and $c_0 = 0.0213$.

The results of the integration are shown in figure 3. The dashed lines in figure 3(a) for $x < 180$ show the envelope obtained from integrating equations (3.1) and the solid lines show the exact wavepacket solution from figure 2(c). The values for the Riemann invariants obtained from the integration are also shown in figure 3(b). The numerical integration failed for $|r_2 - r_3| < 10^{-8}$ which corresponds to the $m = 1$ solitary wave limit and at the point $r_2 = r_3$ the solution is likely discontinuous. Whitham [12] found that the non-rotating equations can have discontinuities across characteristics and these discontinuities can take the form of a jump from a solitary wave to a state of no waves, exactly as seen here in front of the leading solitary wave at $x \approx 180$.

In the limit $m \to 1$, it can be shown $r_1 \to 2d$ and $r_2, r_3, \to 2d + a$ with their characteristic velocities given by $Q_1 \to d$ and $Q_2, Q_3, \to d + a/3$ [13]. If a no wave solution is required ahead of the leading solitary wave then $a = 0$, and r_2 and r_3 must jump to the r_1 solution at the leading edge of the solitary wave. Therefore only r_1 is continuous across this front. Additionally in the limit $m \to 1$ it can be shown $2A \to c_0 d^2 - 2d^3/3$. Hence for a localised solution $d \to 0$ as $|X| \to \infty$, the constant A_0 in (3.2) must be zero because of the zero mass constraint $D \to 0$ as $|X| \to \infty$.

Substituting the above into equation (3.1) gives,

$$\frac{\mathrm{d}\,d}{\mathrm{d}X} = -\frac{\sqrt{c_0 d^2 - 2d^3/3}}{(d - c_0)} \quad \text{for} \quad X > 0, \tag{3.3}$$

which has the solution,

$$X + X_0 = -\sqrt{9c_0 - 6d} + \sqrt{c_0} \log\left[\frac{\sqrt{9c_0 - 6d} + \sqrt{9c_0}}{\sqrt{9c_0 - 6d} - \sqrt{9c_0}}\right], \tag{3.4}$$

where X_0 is a constant. The solution (3.4) is plotted for $x > 180$ in figure 3 where the constant X_0 was fixed using the solution from figure 2(c). Note in figure 3(b) that whilst d is continuous across the edge of the leading solitary wave, its derivative is not. At the point $r_2 = r_3$ (depicted by the vertical dotted line), d has infinite gradient.

For a steady solution with $c = c_0$, the identity $\partial \log \lambda / \partial r_i = 1/6(Q_i - c_0)$ allows the modulation equations (3.1) to be written as the gradient flow

$$\frac{\mathrm{d}\,\boldsymbol{r}}{\mathrm{d}X} = 12D(r_1, r_2, r_3)\nabla_{\boldsymbol{r}} \log \lambda(r_1, r_2, r_3), \tag{3.5}$$

where $\nabla_{\boldsymbol{r}} = (\partial/\partial r_1, \partial/\partial r_2, \partial/\partial r_3)$ and $\boldsymbol{r} = r_1\hat{\mathbf{e}}_1 + r_2\hat{\mathbf{e}}_2 + r_3\hat{\mathbf{e}}_3$ is a point in (r_1, r_2, r_3) space. Since $(\hat{\mathbf{e}}_1 + \hat{\mathbf{e}}_2 + \hat{\mathbf{e}}_3) \cdot \nabla_{\boldsymbol{r}} \log \lambda = 0$ the flow in X is constrained to the plane $r_1 + r_2 + r_3 = 6c_0$ and so has only two degrees of freedom. For a localised solution, $D = \mathrm{sgn}(X)\sqrt{2A}$, and it can be shown that $A = (3c_0 - r_1)(3c_0 - r_2)(3c_0 - r_3)$. The symmetry condition $D(0) = 0$, then implies that one of the Riemann invariants equals $3c_0$ at $X = 0$. For $c_0 > 0$ and distinct $r_i(0)$, the restriction $0 \leq m \leq 1$ means that the only possibility is $r_2(0) = 3c_0$. Either side of $X = 0$ the function D is single signed and bounded away from zero and thus affects simply the speed at which a point moves along the flow lines. Figure 4 shows the trajectories (for $X > 0$, with arrowheads in the direction of increasing X) projected onto the plane $r_2 = 0$. The flow is bounded by the lines $r_3 = (6c_0 - r_1)/2$ and $r_3 = 3c_0 - r_1$ corresponding to $m = 1$ and $r_2 = 3c_0$ respectively. Figure 4 shows that any trajectory starting in this sector moves to $m = 1$ and hence the wave train part of the solution terminates in solitons. The condition $r_2(0) = 3c_0$ also means that solutions satisfy $u_{min} = 0$ at $X = 0$ as observed in the numerical solutions. The bold (red online) line in figure 4 shows the trajectory of the solution in figure 3.

In this section it was shown that the modulation equations accurately describe the wavepacket solution shown in figure 2(c). Although not shown here, the equations were also found to describe the solution shown in 2(b) to a similar degree of accuracy.

(b) Normal dispersion

In contrast to the anomalous case, for normal dispersion there are no known steady wavepacket solutions. Although the wavepacket envelope propagates at a constant velocity, the carrier waves propagate at a velocity different to that of the envelope making the solution intrinsically unsteady. It has also been observed that the phase velocities are non-constant [9]. In the strong-rotation limit, the wavepacket dynamics are described asymptotically by a nonlinear Schrödinger equation bright soliton envelope solution with frequency-shifted linear carrier waves [9]. However in the weak-rotation limit, despite being the most physically relevant parameter range, very little is known about the dynamics of the normal dispersion wavepackets.

For a normal dispersion wavepacket moving at constant velocity, s_0, the time dependence of the modulation equations can be eliminated by moving into the frame $X - s_0 T$. Therefore similarly to the anomalous case, the solution in the translating frame is described by the following equations

$$\frac{\mathrm{d}r_i}{\mathrm{d}X} = \frac{2D}{(Q_i - s_0)}, \quad \text{where} \quad \mathrm{d}D/\mathrm{d}X = d. \tag{3.6}$$

The equations above are identical to the anomalous set (3.1), but with s_0 replacing c_0 and an opposite sign on the right hand side representing the change in dispersion. If the packet is
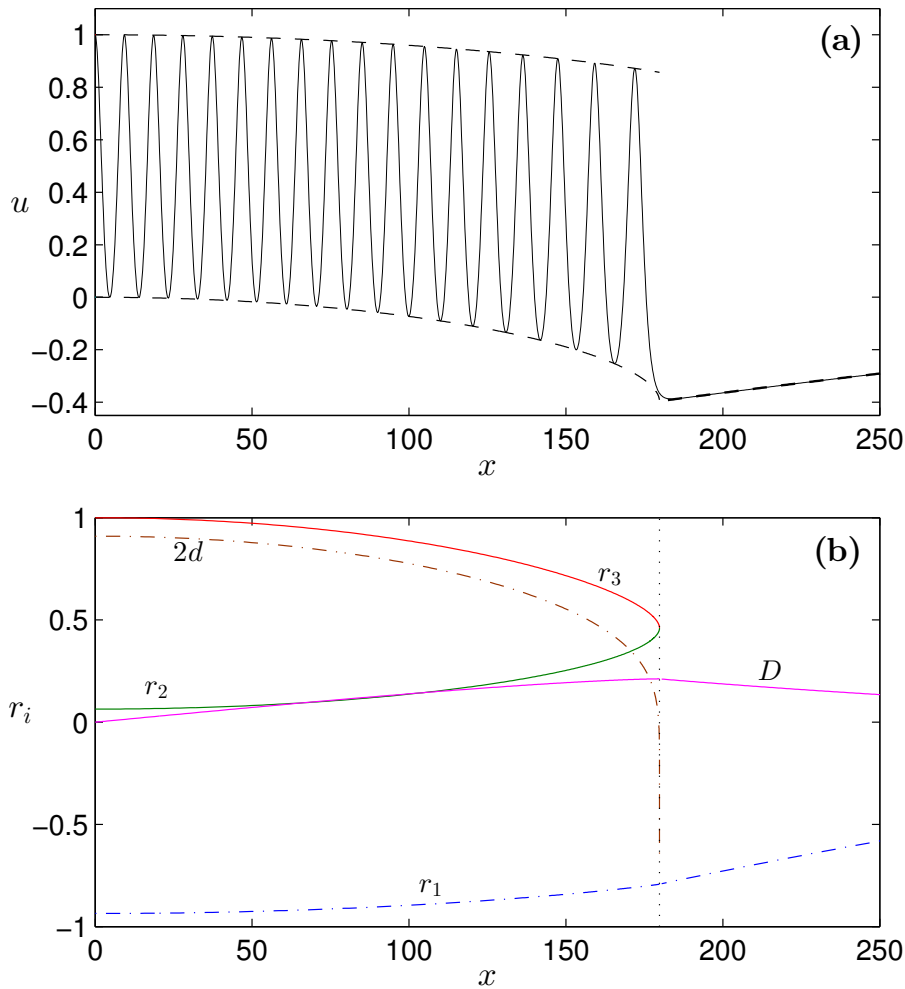
Figure 3. (a) Comparison of the anomalous dispersion wavepacket solution of the Ostrovsky equation (solid line) in figure 2(c) with the modulation equations solution (dashed lines). (b) The Riemann invariants: r_1 (dash-dot line/blue online), r_2 (dashed line/green online), r_3 (solid line/red online) corresponding to the modulation solution in (a). Also shown are D (solid line/magenta online) and $2d$ (dash-dot line/brown online). The vertical dotted line ($x \approx 180$) gives the point where the numerical solution terminates. For $x < 180$ the solution was found by integrating the steady modulation equations with parameters: $\epsilon = 0.00320$, $c_0 = 0.0213$ and initial conditions: $r_1(0) = 3c_0 - 1$, $r_2(0) = 3c_0$, $D(0) = 0$. For $x > 180$ the solution is given by equation (3.4) with $X_0 = -2.0961$.

assumed to be symmetric, forcing $D(0) = 0$, then integrating equation (2.32c) after transforming into the frame, $X - s_0 T$, gives

$$D = -\text{sgn}(X)\sqrt{2(\phi_0 - \phi)}, \tag{3.7}$$

where $\phi = 2A + 2(s_0 - c)(cd + B)$ and ϕ_0 is the value of ϕ at $X = 0$. The sign of the root in (3.7) has been chosen to describe a solution where the "mass" is initially positive when approaching the packet from negative x and hence is opposite in sign to (3.2). For a localised, symmetric wavepacket with normal dispersion, the modulation equations are therefore reduced to a set of three ordinary differential equations. There is one equation more than for the anomalous case as it is not possible to eliminate a Riemann invariant using the expression for c in (2.38).
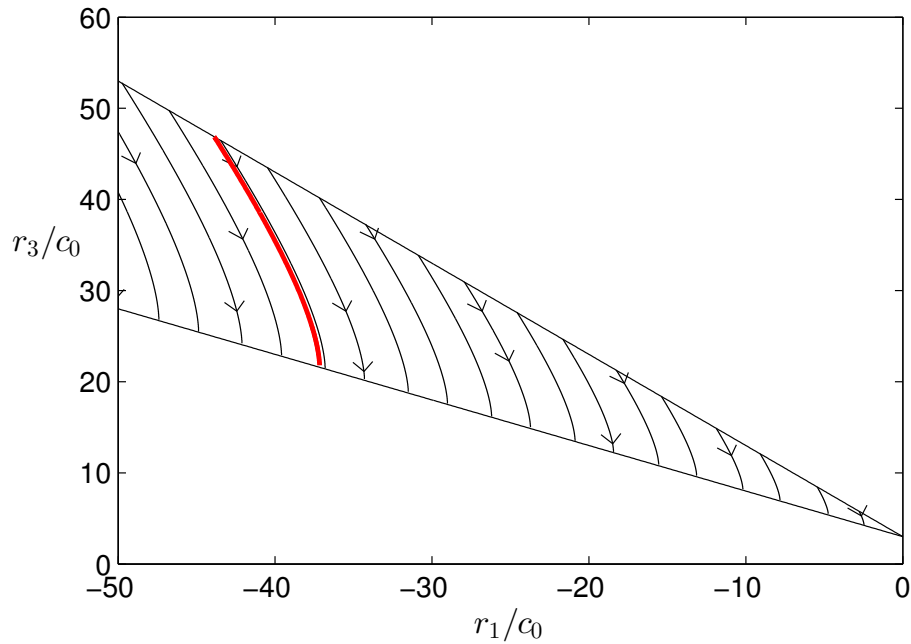
Figure 4. Solution trajectories for a steady solution, $c = c_0$, of the modulation equations with anomalous dispersion in (r_1, r_3) space. The shape of the paths is independent of D which simply changes the speed, i.e. introduces a nonlinear, monotonic stretching in X in the original space. The line $r_3 = (6c - r_1)/2$ corresponds to $m = 1$ and the line $r_3 = 3c - r_1$ corresponds to $r_2(0) = 3c$, i.e. $D = 0$. The bold (red online) line shows the trajectory of the solution of figure 3.

For steady wavepackets with anomalous dispersion it was shown in figure 4 that all solution trajectories travel towards the limit $m = 1$ and terminate in solitary waves. The direction of the trajectories in figure 4 is determined by sign of the dispersion. For wavepackets with normal dispersion it is plausible to predict solution trajectories would move in the opposite direction and travel towards the limit $m = 0$ where they terminate in infinitesimal linear waves. This hypothesis is in agreement with the wavepackets found by Whitfield and Johnson [9], where it was noted that the wavepackets had exponentially small radiating tails at their edges. Under this assumption a solution similar to (3.4) can be found for the outer limit of the wavepacket.

Following Myint and Grimshaw [13] consider the limit $m \to 0$ where $a \to 0$ with a/m fixed and approximately given by $12k^2\beta^2$. In this limit, to leading order in a, it can be shown $r_1 \to 2d - 12k^2\beta^2$, $r_2 \to 2d - 12k^2\beta^2$ and $r_3, \to 2d$ with characteristic velocities given by $Q_1, Q_2 \to d - 12k^2\beta^2$ and $Q_3, \to d$ [13]. Additionally in this limit it can be shown $A \to -2d^2k^2\beta^2 + d^3/6$, $B \to 4dk^2\beta^2 - d^2/2$ and $c \to d - 4k^2\beta^2$. Therefore $D^2 = 2\phi_0 - s_0 d^2 + 2d^3/3$ and hence for a localised solution $d \to 0$ as $|X| \to \infty$, the constant ϕ_0 in (3.7) must be zero because of the zero mass constraint $D \to 0$ as $|X| \to \infty$. Substituting these results into equation (3.6) for r_3 gives,

$$\frac{\mathrm{d}\,d}{\mathrm{d}X} = -\frac{\sqrt{2d^3/3 - s_0 d^2}}{(d - s_0)} \quad \text{for} \quad X > 0, \tag{3.8}$$

which has the solution,

$$X + X_0 = -\sqrt{6d - 9s_0} - 2\sqrt{s_0}\arctan\left[\sqrt{\frac{3s_0}{2d - 3s_0}}\right], \tag{3.9}$$

where X_0 is a constant. In the limit $m \to 0$, the solution to leading order in a is given by $u = d$ and hence it is expected that (3.9) would be the solution at the wavepacket edge.

In Whitfield and Johnson [9] numerical solutions were obtained for unsteady wavepackets with normal dispersion. Therefore to test if the modulation equations have wavepacket solutions, equations (3.6) were integrated numerically using an initial condition corresponding to the wavepacket with the weakest rotation in [9]. Using the measured envelope values from [9] approximations for $r_1(0)$, $r_2(0)$ and $r_3(0)$ could be parameterised as a function of $c(0)$. The constant ϕ_0 in (3.7) was assumed to be zero for the reasons outlined in the preceding paragraph and hence imposing the symmetry condition, $D(0) = 0$, fixed the value of s_0 for a given $c(0)$. The lack of data made it impossible to determine $c(0)$ and therefore it was left as a parameter. As was done for anomalous dispersion, the equation $dD/dX = d$, was used to avoid the difficulty of integrating from a stationary point.

The result of one integration is shown in figure 5. In figure 5(a) the dashed lines for $|x| < 60$ show the envelope obtained from numerically integrating equations (3.6) and the dashed lines for $|x| > 100$ show the analytical solution (3.9) with $X_0 = -1.7756$. The dotted lines in figure 5(a) show the measured envelope obtained by Whitfield and Johnson [9] and the solid lines show the exact unsteady solution from [9] at its maximum value. The Riemann invariant values obtained from the integration are also shown in figure 5(b). The value of $c(0)$ in figure 5 was chosen to produce the best agreement with the measured packet envelope however for a wide range of different $c(0)$ it was found that the numerical integration failed before it could reach the edge of the wavepacket. This was because $Q_2 \to s_0$ which led to $|dr_2/dX|$ being extremely large. The reason for this behaviour is unclear. The approximate initial conditions are a possible source of error, as is the assumption of a symmetric solution, especially as it was shown conclusively in [9] that for $\epsilon \gg 1$ wavepackets had asymmetry of order $1/\epsilon$.

When the localised solution condition was relaxed allowing $\phi_0 \neq 0$, it was possible to choose initial values such that the numerical integration for the modulation equations would not fail. Using the initial conditions of the wavepacket solution shown in figure 5 as a starting point, the values of s and $c(0)$ were varied until a numerical integration was found such that $Q_2 \to s_0$ was avoided. The results of one of these integrations are shown in figure 6. Figure 6 shows a periodic solution of the modulation equations, suggesting the Ostrovsky equation possesses unsteady, periodically modulated cnoildal wave solutions such that the modulation is steady in the frame $x - st$. The shape of periodic packets shown in figure 6(a) are similar to that of figure 6(b). Both solutions have the same value of u_{max} and u_{min} and consequently the first three digits of the Riemann invariant initial conditions are identical.

Previous works have suggested the rotation-induced wavepackets shown in figure 5(a) could describe why non-rank-ordered internal solitary wavepackets are sometimes observed instead of the expected rank-ordered wavepacket structure of the non-rotating KdV case [18]. The solution shown in figure 6(a) provides further evidence that rotational effects influence internal wavetrains in such a way that they form non-rank-ordered packet structures. However the question of whether the solution shown in figure 6(a) arises in the Ostrovsky equation from general initial conditions is still unclear.

4. Wavepacket emergence

The variables and analysis of §3 give a context for discussing the emergence of the wavepacket solutions above from KdV soliton initial conditions under weak rotation as observed by Grimshaw and Helfrich [8], Grimshaw et al. [7] and Whitfield and Johnson [9]. In terms of the variables (2.4), equation (2.1) has the inner solitary wave solution,

$$u^i = a \operatorname{sech}^2[(a/12)^{1/2}(x - c(T)t)] + \epsilon d(T) + \mathcal{O}(\epsilon^2), \tag{4.1}$$

where $c(T) = \frac{1}{3}a + \epsilon d(T)$ gives the slowly- and weakly-varying speed of the solitary wave on a small, slowly-varying pedestal. For a KdV soliton initial condition of amplitude a_0, $a = a_0$ and $d(0) = 0$. As $x \to \pm\infty$, $u^i \to \epsilon d(T)$ and so merges smoothly onto an outer solution $u = \epsilon u^o(X, T)$,
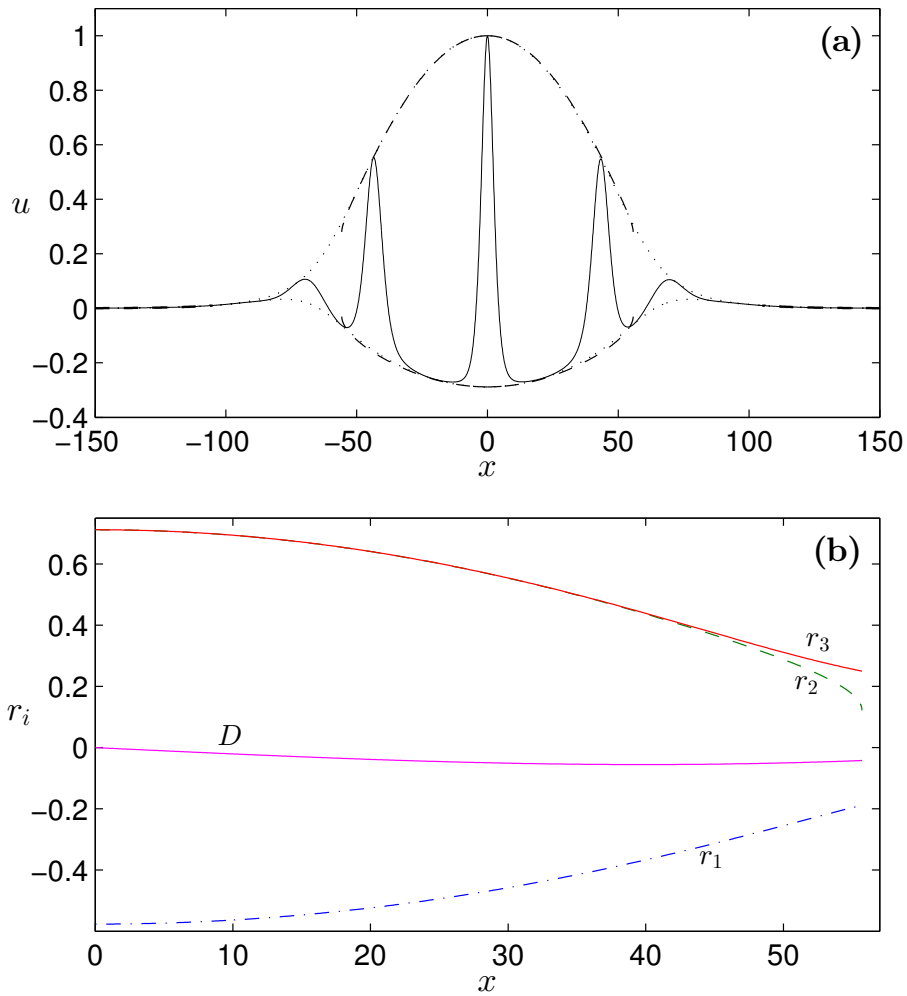
Figure 5. (a) An unsteady, normal-dispersion wavepacket solution of the Ostrovsky equation (solid line) and its envelope (dotted lines) compared with the modulation equations solution (dashed lines). (b) The Riemann invariants: r_1 (dash-dot line/blue online), r_2 (dashed line/green online), r_3 (solid line/red online) and D (solid line/magenta online) for the modulation solution in (a). For $|x| < 60$ the solution was found by integrating the steady modulation equations with parameters: $\epsilon = 0.0180$, $s = -0.0696184455926651$ and initial conditions: $r_1(0) = -0.5764950170104435$, $r_2(0) = 0.7117495206851349$, $r_3(0) = 0.7117554623044217$, $D(0) = 0$. For $|x| > 100$ the solution is given by equation (3.9) with $X_0 = -1.7756$.

which satisfies, to leading order in ϵ

$$u^o_{TX} = \pm u^o. \tag{4.2}$$

At this order the speed c can be taken to be constant with $c = c_o = a/3 > 0$. Moving to a frame translating to the right with speed c_0 by writing $\xi = X - c_0 T$, gives

$$u^o_{T\xi} - c_0 u^o_{\xi\xi} = \pm u^o, \qquad \xi \neq 0, \tag{4.3a}$$

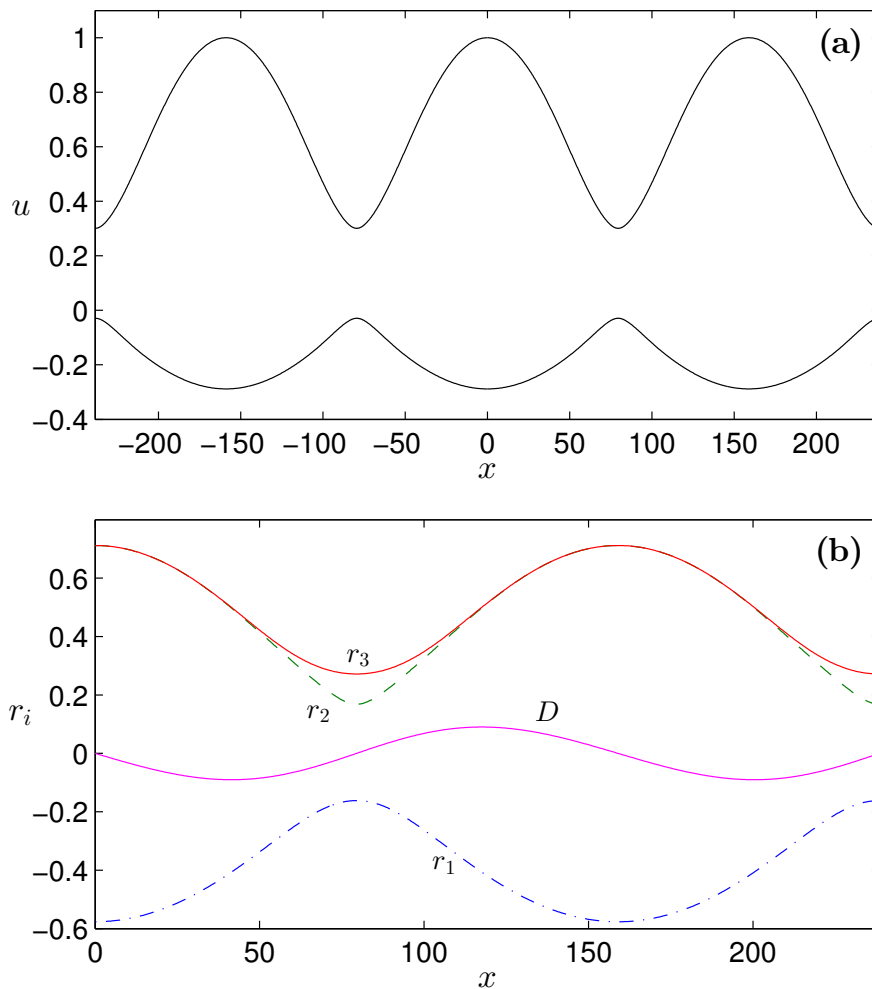$$u^o(0, T) = d(T). \tag{4.3b}$$

Figure 6. (a)A periodic wavepacket solution of the modulation equations with normal dispersion. (b) The Riemann invariants: r_1 (dash-dot line/blue online), r_2 (dash-dot line/green online), r_3 (solid line/red online) and D (solid line/magenta online) for the solution in (a). The solution was obtained by integrating the steady modulation equations with $\epsilon = 0.0180$, $s = -0.0789$ and initial conditions $r_1(0) = -0.5765278735351373$, $r_2(0) = 0.7117166641604410$, $r_3(0) = 0.7117554623044217$, $D(0) = 0$.

The problem is closed at this order by the mass constraint (1.3) which gives, to leading order,

$$\int_{-\infty}^{\infty} a_0 \operatorname{sech}^2((a_0/12)^{1/2}\theta)\, \mathrm{d}\theta + \int_{-\infty}^{\infty} u^o\, \mathrm{d}\xi = 0, \tag{4.4a}$$

i.e. $\qquad [c_0 u_\xi^o]_0 = \pm A, \tag{4.4b}$

using (4.3), where $[\,]_0$ denotes the jump in the enclosed quantity across $\xi = 0$ and $A = 4\sqrt{3/a_0}$. In particular, (4.3a) becomes the forced linearised reduced Ostrovsky equation

$$u_{T\xi}^o - c_0 u_{\xi\xi}^o \mp u^o = \pm A\delta(\xi), \tag{4.5}$$

where $\delta(\xi)$ denotes the Dirac delta function. Writing

$$u^o(\xi, T) = \int_{-\infty}^{\infty} \hat{u}(\kappa, T)\mathrm{e}^{\mathrm{i}\kappa\xi}\, \mathrm{d}\xi, \tag{4.6}$$
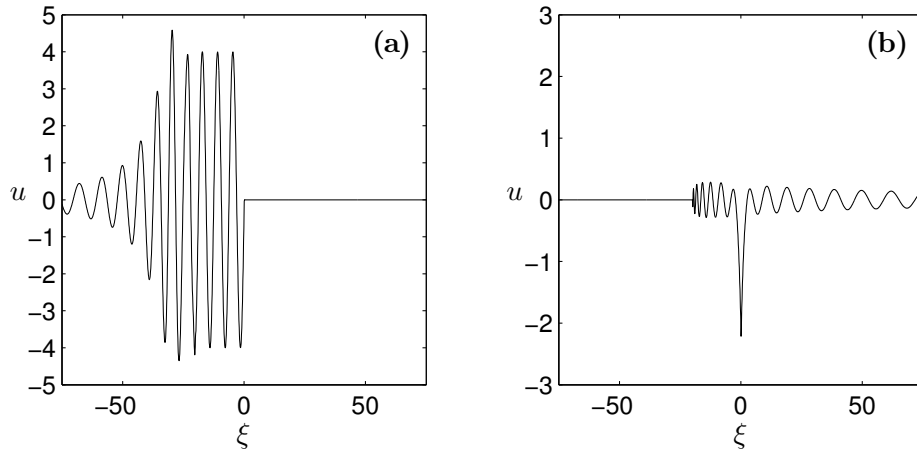
Figure 7. The outer solution of (4.5) at time $T = 20$, for speed $c_0 = 1$ and amplitude $A = 4$, shown in a frame moving with the soliton. (a) Normal dispersion. The steady lee-wave wake has been established in $-20 < \xi < 0$ with transients in $\xi < -20$. (b) Anomalous dispersion. Transients occupy the region $\xi > -20$ with the steady response established at the origin.

gives the Fourier transform of (4.5) as

$$\hat{u}_T + i\omega(\kappa)\hat{u} = \pm A/i\kappa, \tag{4.7}$$

where $\omega(\kappa) = -c_0\kappa \pm 1/\kappa$, with solution vanishing at $T = 0$,

$$\hat{u}(\kappa, T) = A(e^{-i\omega T} - 1)/(1 \mp c_0\kappa^2). \tag{4.8}$$

The solution consists of the steady solution forced by the poles at $\kappa^2 = \pm 1/c_0$ and a superposition of dispersive waves of frequency $\omega(\kappa)$ and group velocity $c_g(\kappa) = -c_0 \mp 1/\kappa^2$. The flow evolution and final state for normal and anomalous dispersion differ.

For normal dispersion c_g is strictly negative for all κ and all waves propagate in the negative ξ direction. The poles in (4.7), (4.8) lie on the real κ axis and thus contribute a steady downstream lee-wave train behind the soliton with the deviation of the solution from its final steady state decaying as $T^{-1/2}$ at large T, so that as $T \to \infty$

$$u \to \begin{cases} \mathcal{O}(T^{-1/2}) & \xi > 0, \\ (A/\sqrt{c_0})\sin(\xi/\sqrt{c_0}) + \mathcal{O}(T^{-1/2}) & \xi < 0, \end{cases} \tag{4.9}$$

as in figure 7(a). There is an order ϵ^2 momentum flux in the negative X-direction in the lee of the soliton which exerts a drag on the soliton, leading to a decay in the soliton over the longer timescale $\epsilon T = \epsilon^2 t$. This longer-time decay of the soliton is discussed in greater detail by Grimshaw et al. [19] and Grimshaw et al. [7].

For anomalous dispersion the poles in (4.7), (4.8) lie on the imaginary κ axis and thus contribute a symmetric steady contribution decaying exponentially away from a maximum at $\xi = 0$. The group velocity vanishes when $\kappa^2 = c_0$. Thus transient long waves with $|\kappa| < c_0^{-1/2}$ propagate to $\xi = \infty$ in advance of the soliton, decaying as $T^{-1/2}$, while transient short waves with $|\kappa| > c_0^{-1/2}$ propagate to $\xi = -\infty$ in the lee of the soliton, decaying as $T^{-1/2}$. Waves with $|\kappa| = c_0^{-1/2}$ remain in vicinity of the soliton. As $dc_g/d\kappa = 2/\kappa^3$ vanishes nowhere, these waves decay as $T^{-1/3}$. Thus, as $T \to \infty$,

$$u \to (-A/2\sqrt{c_0})\exp(-|\xi|/\sqrt{c_0}) + \mathcal{O}(T^{-1/3}), \tag{4.10}$$

as in figure 7(b). The final flow state is symmetric without waves and so suffers no wave drag. Unlike the case of normal dispersion there is no further leading order evolution over the longer timescale $\epsilon T = \epsilon^2 t$, in agreement with the numerical integrations of [7]. Note that although the $T \to \infty$ asymptotic state is a symmetric zero-drag solution, the solution is asymmetric throughout the evolution to this state and so the soliton suffers a loss of momentum flux of order ϵ^2, leading to a reduction in its amplitude. This higher-order effect is not captured by leading order analysis here. The departure from the analysis in [7], which leads to the prediction of a decaying soliton there, is that the far-field boundary condition on the leading order solution $u^{(0)}$ of [7], compatible with (4.10), is $u^{(1)}(\theta \to -\infty) = u^{(1)}(\theta \to +\infty)$, so $u^{(1)} =$ constant is an allowable solution of the adjoint equation (3.9) of [7], giving conservation of mass to leading order in γ.

5. Discussion

The Whitham modulation equations for the Ostrovsky equation, derived using the method of Myint and Grimshaw [13], have been used to find wavepacket solutions of the Ostrovsky equation in the weak-rotation limit. Considering wavepacket solutions in the modulation equations offers two advantages: first, the anti derivative representing large-scale dispersion is simplified to an algebraic term and second, intrinsically unsteady wavepacket solutions of the Ostrovsky equation with normal dispersion, whose phase and group velocities differ, become steady solutions.

For anomalous dispersion a new type of cnoidal wavepacket solution was obtained and shown to be representable as a solution of the modulation equations. The modulation equations showed, in agreement with numerical integrations, that the wavepacket has minimum zero at its centre and that the wave train section of the packet terminates in a KdV soliton at each edge. An analytical solution for the outer section of the wavepacket where no waves exist was also found.

In contrast to the anomalous dispersion case, for normal dispersion it is argued that any localised symmetric wave train solution should approach infinitesimal linear waves at its edge and more solitary-like waves at its centre. Based on this assumption an analytical solution for the outer limit of the wavepacket was found. The outer solution was compared with data from a normal dispersion wavepacket found in [9], showing good agreement. The same packet data was also compared with solutions of the modulation equations for the inner wave train region of the packet and agreed well over the central partion of the packet. Towards the edge of the packet, the characteristic velocity of the intermediate Riemann invariant became equal to the packet propagation speed introducing an infinite gradient in the integrations across the packet. This singularity appears to be a robust feature of the equations when applied to these packets but its physical meaning has not been determined. The good agreement of the modulation solution with the data over the majority of the wavepacket suggests that the modulation equations do have wavepacket solutions for normal dispersion, supporting the observation of Helfrich [11] that the wavepackets under normal dispersion can be regarded as modulated cnoidal waves.

Section 4 decribes the emergence of these wavepackets from KdV soliton initial conditions under weak rotation. For anomalous dispersion the flow adjusts over times of order ϵ^{-1} to a zero-drag symmetric state that undergoes no futher evolution at this order. For normal dispersion the flow evolves over times of order ϵ^{-1} to an asymmetric non-zero drag form that undergoes further slow decay over times of order ϵ^{-2}, as described by Grimshaw et al. [19].

For the Ostrovsky equation with normal dispersion it is known cnoidal wavepacket solutions arise from localised initial conditions. Future work is needed to determine whether the same is also true for the new type of cnoidal wavepacket found in this paper for the Ostrovsky equation with anomalous dispersion.

Ethics. This does not apply to our paper.

Data Accessibility. This work has no data.

Authors' Contributions. The authors are equally responsible for the contributions to the paper and both authors gave final approval for publication.

Competing Interests. We have no competing interests.

References

1 Ostrovsky LA, Stepanyants YA. Do internal solitions exist in the ocean? Reviews of Geophysics. 1989;27(3):293–310.

2 Grimshaw RHJ. Internal Solitary Waves. In: Liu PLF, editor. Advances in Coastal and Ocean Engineering. World Scientific Publishing Company, Incorporated; 1997. p. 1–30.

3 Helfrich KR, Melville WK. Long nonlinear internal waves. Annu Rev Fluid Mech. 2006;38:395–425.

4 Apel JR, Ostrovsky LA, Stepanyants YA, Lynch JF. Internal solitons in the ocean and their effect on underwater sound. The Journal of the Acoustical Society of America. 2007;121(2):695–722.

5 Ostrovsky LA. Nonlinear internal waves in a rotating ocean. Oceanology. 1978;18:199–125.

6 Nikitenkova S, Singh N, Stepanyants Y. Modulational stability of weakly nonlinear wave-trains in media with small-and large-scale dispersions. Chaos: An Interdisciplinary Journal of Nonlinear Science. 2015;25(12):123113.

7 Grimshaw RHJ, Stepanyants YA, Alias A. Formation of wave packets in the Ostrovsky equation for both normal and anomalous dispersion. Proceedings of the Royal Society of London A: Mathematical, Physical and Engineering Sciences. 2016;472(2185):20150416.

8 Grimshaw RHJ, Helfrich KR. Long-time Solutions of the Ostrovsky Equation. Studies in Applied Mathematics. 2008;121(1):71–88.

9 Whitfield A, Johnson E. Rotation-induced nonlinear wavepackets in internal waves. Physics of Fluids (1994-present). 2014;26(5):056606.

10 Whitfield AJ, Johnson ER. Wave-packet formation at the zero-dispersion point in the Gardner-Ostrovsky equation. Phys Rev E. 2015 May;91:051201.

11 Helfrich KR. Decay and return of internal solitary waves with rotation. Physics of Fluids. 2007;19(2):026601.

12 Whitham GB. Linear and nonlinear waves. vol. 42. John Wiley & Sons; 2011.

13 Myint S, Grimshaw RHJ. The modulation of nonlinear periodic wavetrains by dissipative terms in the Korteweg-de Vries equation. Wave Motion. 1995;22(2):215–238.

14 Kamchatnov AM. On Whitham theory for perturbed integrable equations. Physica D: Nonlinear Phenomena. 2004;188(3):247–261.

15 Hunter JK. Numerical solutions of some nonlinear dispersive wave equations. Lect Appl Math. 1990;26:301–316.

16 Obregon M, Stepanyants YA. Oblique magneto-acoustic solitons in a rotating plasma. Physics Letters A. 1998;249(4):315–323.

17 Vlasenko V, Sanchez Garrido JC, Stashchuk N, Garcia Lafuente J, Losada M. Three-Dimensional Evolution of Large-Amplitude Internal Waves in the Strait of Gibraltar. Journal of Physical Oceanography. 2009;39(9):199–125.

18 Grimshaw RHJ, Helfrich KR, Johnson ER. Experimental study of the effect of rotation on nonlinear internal waves. Physics of Fluids (1994-present). 2013;25(5):056602.

19 Grimshaw RHJ, He JM, Ostrovsky LA. Terminal damping of a solitary wave due to radiation in rotational systems. Stud Appl Math. 1998;101:197–210.